Optimization and Flight Test Results of Modern Control Laws for the UH-60 Black Hawk

Mark B. Tischler and Chris L. Blanken
mtischler@mail.arc.nasa.gov/cblanken@mail.arc.nasa.gov
Army/NASA Rotorcraft Division, Aeroflightdynamics Directorate
U.S. Army Aviation and Missile Research, Development, and Engineering Center
Ames Research Center, Moffett Field, CA

Kenny K. Cheung
kcheung@mail.arc.nasa.gov
Raytheon ITSS
Ames Research Center, Moffett Field, CA

Sean S. M. Swei
Sswei@mail.arc.nasa.gov
AerospaceComputing, Inc.
Ames Research Center, Moffett Field, CA

Vineet Sahasrabudhe and Alexander Faynberg
Vsahasrabudhe@sikorsky.com/Afaynberg@sikorsky.com
Sikorsky Aircraft Corporation, Stratford, CT

ABSTRACT

Modern control laws (MCLAWS-2) were developed to provide an attitude-command/attitude-hold response type for the UH-60, and thereby afford improved handling-qualities for near-Earth operation in night and poor weather. The MCLAWS-2 were implemented and evaluated in an EH-60L helicopter. Central to addressing the significant resource and technical challenges of this project was the extensive use of a modern integrated toolset. System identification methods provided an accurate flight-identified aircraft response model, and allowed the efficient isolation of discrepancies in the block diagram-based simulation model. Additional key tools were real-time rapid prototyping and a well-designed picture-to-code process. Control laws were tuned to achieve the maximum design margin relative to handling-qualities and control system performance requirements. The optimized design was seen to be robust to uncertainties in the identified physical parameters. A flight test evaluation by three test pilots showed significant benefits of the optimized design compared to the EH-60L standard flight control configuration.

Presented at the AHS 4th Decennial Specialists' Conference on Aeromechanics, San Francisco, CA, 21-23 January 2004.

INTRODUCTION

Sikorsky Aircraft Corporation (SAC), under a National Rotorcraft Technology Center (NRTC) project, is developing modernized flight control laws for legacy aircraft that operate in the degraded visual environment. The baseline aircraft for this effort is the UH-60 Black Hawk helicopter. These control laws are aimed at providing an attitude-command/attitude-hold (ACAH) control response using the existing partial authority flight control augmentation actuation system. An ACAH control response is an essential element in retaining satisfactory handling qualities for near-Earth operations as the pilot's visual cues degrade, such as for night and poor weather operations (Ref. 1). The initial design of these modernized control laws uses only the inner-loop Stability Augmentation System (SAS) servos to implement the ACAH response type and are referred to as MCLAWS-2 (read as "MCLAWS minus-two"). The outer-loop trim servos will be incorporated into the next version (MCLAWS-1) to help re-center the SAS servos and minimize saturation. The final version of the control laws, denoted as MCLAWS, will have an additional linear acceleration feedback loop that further improves performance in the presence of winds and gusts.

The MCLAWS-2 were first assessed in ground-based piloted simulations at both Sikorsky and the NASA-Ames Vertical Motion Simulator (VMS). One of the key results from these ground-based simulations (Ref. 2) was that the ACAH response in pitch and roll improved the handling qualities in the hover/low speed flight regime. Also, the improvements found were consistent across a range of mission task elements (MTEs) for both the good and degraded visual environment. To extend the simulation results and reduce the risk for implementation onto production aircraft, a flight test assessment was undertaken and performed in cooperation with Sikorsky on the Army/NASA EH-60L Black Hawk helicopter[1]. The initial flight assessment reported herein was performed in the daytime with a good visual environment. The objective was to evaluate the MCLAWS-2 on a Black Hawk using the existing Stability Augmentation System (SAS) partial authority servos. These servos provide ±10% authority relative to the pilot's control[2]. For the flight test, the approach was to initially compare and validate the control law responses between simulation and flight, and, if necessary, re-optimize the control law gains to account for observed modeling discrepancies and aircraft implementation issues. Once optimized, the team performed a handling quality evaluation using Aeronautical Design Standard–33 (Ref. 1).

The design, optimization, and flight testing of the modern partial authority control laws on the EH-60L constituted both resource and technical challenges. The resource challenges of project schedule and limited number of available flight test hours placed a significant emphasis on tools for the accurate simulation of dynamic response and rapid prototyping. The technical challenge of meeting multiple competing design objectives (e.g., short-term response, stability, disturbance rejection, degree of saturation) within the limited (±10%) available SAS control authority and significant hardware system lags was met using optimization-based control system design methods. Central to addressing these challenges, and the focus of this paper, was the extensive use of a modern integrated tool set.

The key elements of the integrated tool set were: block diagram simulation (Simulink® (Ref. 3)), system identification (CIFER® (Ref. 4)), control system analysis and optimization (CONDUIT® (Ref. 5)), real-time rapid prototyping (RIPTIDE (Ref. 6)), and pictures-to-code conversion. A detailed block diagram model of the partial authority system implementation in the EH-60L was developed in Simulink® as the basis for control law analysis and optimization. Central to the simulation was an accurate flight dynamics model of the UH-60 airframe obtained from frequency-domain system identification studies (Ref. 7) using the Comprehensive Identification from Frequency Responses (CIFER®) facility. CIFER® was also used extensively to isolate and correct modeling discrepancies based on subsystem and end-to-end frequency-response comparisons of the simulation versus the EH-60L flight data. Control law evaluation and optimization was completed using the Control

[1] The actual test aircraft was a prototype EH-60L Advance QuickFix aircraft that was modified for flight testing. All external antennas and aircraft survivability equipment were removed from the aircraft making the external airframe similar to a standard UH-60L. The test aircraft was operated with the directional and vertical gyros providing inputs to the flight control system to provide the same aircraft response as a standard UH-60L.

[2] By convention, cockpit stick throw has a range of 0-100% corresponding to 0-10 in. of travel. Maximum command of the SAS produces ±1 in. equivalent stick motion, which is referred to as a ±10% authority system.

Designer's Unified Interface (CONDUIT®), which proved an effective tool to rapidly reach a design solution that met the competing objectives with minimum overdesign. Control laws were implemented using pictures-to-code techniques (MATLAB Real-Time Workshop Embedded Code Generation (Ref. 8)) to eliminate hand coding of control system block diagrams and updates. Final control-law checkout and piloted evaluation of the MCLAWS-2 control law implementation prior to flight was conducted using the Real Time Interactive Prototype Technology Integration Development Environment (RIPTIDE).

This paper presents the methodology and results of using the integrated tool set for development, optimization, and flight testing of the MCLAWS-2 for the EH-60L. First, an overview is presented of the MCLAWS-2 concept and hardware implementation on the EH-60L aircraft. The next section presents the analysis methods used for modeling, control system evaluation, and model discrepancy isolation. Example results of the corrected model show excellent agreement with the system identification flight test data for a baseline gain set. The isolation of modeling discrepancies in the individual hardware blocks and the numerical buildup of broken-loop flight response using system identification techniques are unique aspects of this paper. Next, handling-qualities analyses and control system optimization using CONDUIT® are explained in detail. Optimization based on "design margin" is shown to provide a family of designs based on uniformly increasing performance. This design approach is validated with the flight results. The robustness analysis based on the uncertainty bounds of the identified physical model parameters and the identification model structure is also a unique aspect of this paper. The final section covers the flight evaluation of the optimized MCLAW-2 configuration, showing significant qualitative and quantitative performance benefits compared to the EH-60L standard SAS/Flight Path Stabilization (FPS) flight control system.

MCLAWS-2 CONCEPT AND IMPLEMENTATION

The basic structure of the Modern Control Laws (MCLAWS-2) investigated in this study is shown in Fig. 1. The figure shows the pitch-axis structure only; the roll and yaw axes have a similar structure. Also shown for comparison is the structure of the current pitch-axis control laws that are part of the Stability Augmentation System (SAS) on current UH-60A aircraft. The current pitch SAS is essentially a rate feedback system that augments the damping of the bare airframe dynamics.

The principal objective of MCLAWS is to provide the pilot with an ACAH response type. However, in a partial authority system, this places a challenge on the design of the control laws to operate without saturating the SAS servo authority limit. While transiently touching the limits may be acceptable, especially during

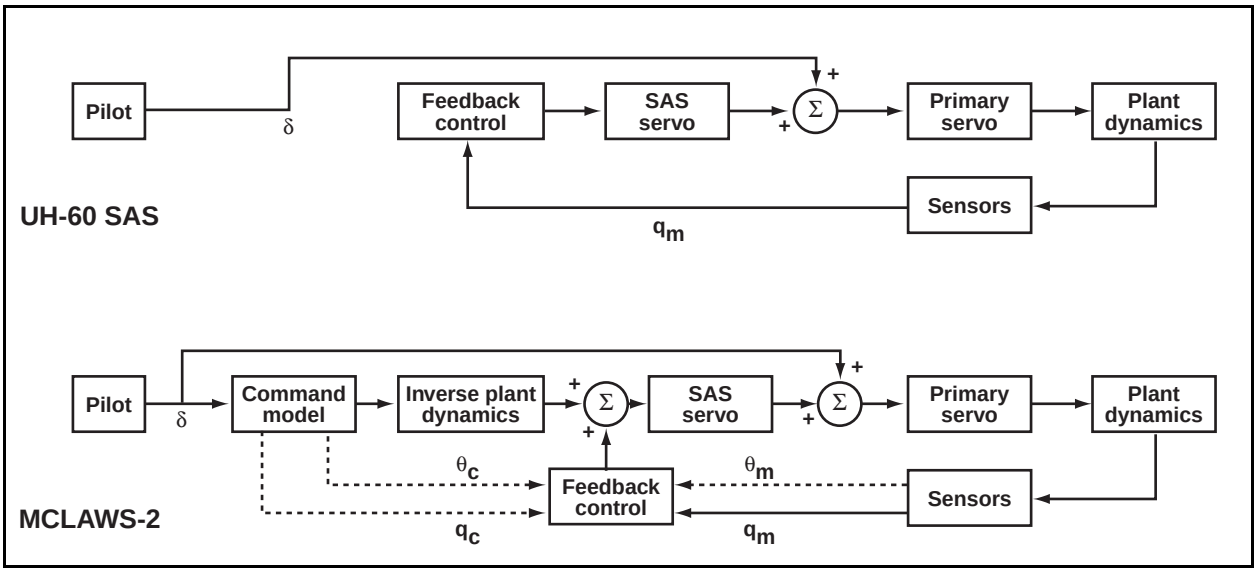

Figure 1. Standard UH-60 and MCLAWS schematic diagrams.

maneuvers, prolonged saturation leaves the helicopter with no augmentation whatsoever. It may be possible to use the trim servos to help keep the SAS servos centered and reduce saturation, but this may result in undesirable stick motions being seen by the pilot. The challenge addressed here is the implementation of such control laws in existing aircraft with constraints on SAS authority limits, sensor complement, and computational power.

The MCLAWS-2 implements a two-mode control system. In the attitude mode the pitch and roll axes have ACAH type responses, while the yaw axis has rate-command/direction-hold (RCDH) characteristics. The pitch and roll control laws switch to a rate command mode if the helicopter velocities or attitudes exceed the limits shown in Table 1. As the name indicates, in the rate mode the aircraft has a Rate Command (RC) response type. In order to switch back to attitude mode from rate mode, more restrictive conditions must be met which are also shown in Table 1. Recall that in this study the MCLAWS-2 were implemented using only the inner-loop SAS servos. When the system switches from attitude mode to rate mode, the dashed paths in Fig. 1 are removed gracefully, and the systems revert back to a rate feedback architecture almost identical to the baseline UH-60A SAS control laws. Conversely, when the aircraft re-enters the attitude mode, these paths are brought back in gradually. The overall objective was to retain ACAH characteristics over a useful range of aircraft velocities and attitudes without persistently saturating the SAS.

Table 1. Attitude to rate mode switching thresholds.

	ACAH will engage if:	ACAH will disengage if:
$\lvert\theta\rvert$	<15 degrees, and	>25 degrees, or
$\lvert\phi\rvert$	<10 degrees, and	>35 degrees, or
$\sqrt{U^2+V^2}$	<20 knots	>30 knots

The initial gain set (referred to herein as "*baseline*") for the MCLAWS-2 flight-test effort was based on linear analysis, extensive non-linear piloted simulation (as described in Ref. 2), and an initial analysis using CONDUIT®. A check of these gains using an identified model of the test aircraft (Ref. 7) indicated satisfactory performance for a range of stability and handling qualities requirements.

EH-60L INTEGRATION

The implementation of the MCLAWS-2 onto the Army/NASA EH-60L helicopter included the installation of a research flight control computer (RFCC), a switch for selection between the EH-60 standard SAS or the RFCC, and features to ensure satisfactory engagement/disengagement of the RFCC. For example, interlock features were designed into the system to prevent engagement if the RFCC is not functioning properly or if the aircraft air data system is not available. In addition, dummy electrical loads were switched in for servos to satisfy the EH-60 stability augmentation system and flight path system (SAS/FPS) monitors so that reversion from the RFCC was to the standard EH-60 SAS with trim on. The RFCC was engaged in the air, with all take-offs and landings performed with the standard EH-60 SAS/FPS. Fig. 2 shows a picture of the aircraft data system operator's station on the left side and the research flight control computer and operator station on the right side.

Figure 2. Photograph of Army/NASA EH-60L cabin with air data system and research flight control computer console stations.

A key aspect of the integration was the ease with which the modern control laws could be transferred between Sikorsky and the Army Aeroflightdynamics Directorate (AFDD), analyzed, simulated on the ground prior to flight, and transferred onto the aircraft. MATLAB®/Simulink® control law block diagrams were central to this process (Fig. 3). The pictures-to-code pathway between analysis, simulation tools, and the aircraft used the MATLAB® Real-Time Workshop Embedded Coder for rapid turnaround and very cost-effective design iteration. A final iteration step was the

ability to change some control law parameters on-board the aircraft while in flight. The control laws and proposed modifications were evaluated in the RIPTIDE ground-based simulation environment (Fig. 4) prior to aircraft engagement.

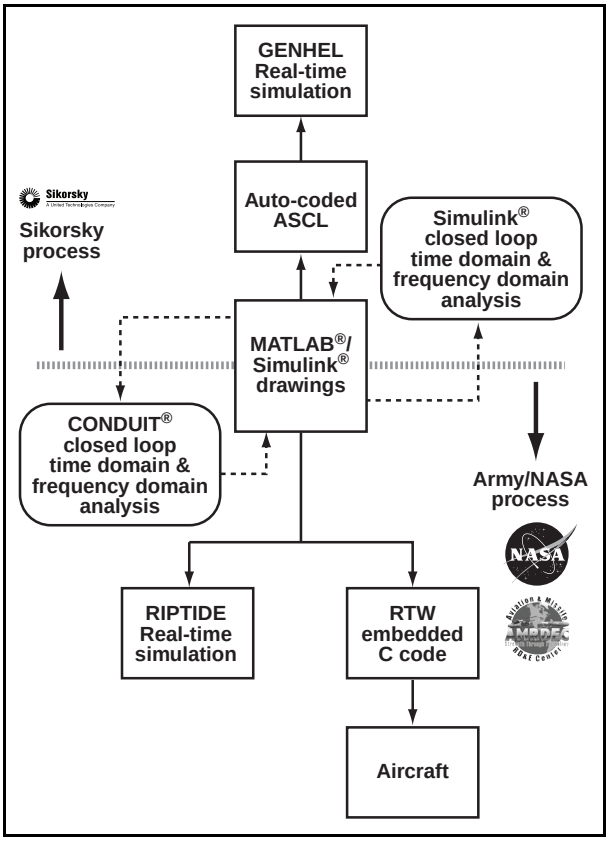

Figure 3. Pictures-to-Code process.

Figure 4. RIPTIDE real-time simulation.

SIMULINK® ANALYSIS MODEL

In parallel with the MCLAWS-2 implementation into the EH-60L, a detailed model of the helicopter and control system was developed in Simulink® (Fig. 5) for analysis and optimization of the ACAH mode in low-speed/hovering flight. This model was initially evaluated using CONDUIT® to document expected broken-loop and closed-loop response characteristics for the baseline set of MCLAWS-2 gains. The Simulink® model for the ACAH control mode was comprised of 91 states, including key elements of:

- Attitude command and feedback loops of the SAS represented by transfer functions (light blue).
- Flight-identified 36-state bare-airframe linear model (light green).
- SAS servo actuators – pitch, roll and yaw channels (yellow).
- Primary servo actuators – pitch, roll, yaw and collective channels (orange).
- Transport (Padé) delay approximation of phase lag contribution by sensor dynamics (red).

The model of the bare-airframe response to mixer input is a central element of the Simulink® simulation and determines to a large extent the overall accuracy of the control system analysis. Fletcher et al. (Ref. 7) extracted an accurate (linear) state-space representation of the JUH-60A dynamics for hover/low-speed flight from flight data using CIFER®:

$$\begin{aligned} M\dot{x} &= Fx + Gu \\ y &= Hx + Ju \end{aligned} \tag{1}$$

The bare airframe model is comprised of 36 states and includes the dynamics of the fuselage, rotor flapping, rotor lead-lag, engine/governor/fuel system, dynamic inflow, and aerodynamic phase lag. The model is valid over the frequency range of 0.5-40 rad/sec, and is well suited for flight control applications (Ref. 9). Other applications of this model have included full authority fly-by-wire flight control design (Ref. 10), gust response modeling (Ref. 11), and envelope limiting and cueing (Ref. 12). An important additional product of the system identification study was the set of 1σ confidence bounds for each identified parameter. These confidence bounds were used to evaluate the robustness of the optimized control system to parameter uncertainty, as discussed later. As part of the integrated toolset, the state-space model and 1σ confidence bounds were retrieved directly from the CIFER® database for use in the Simulink® analysis model.

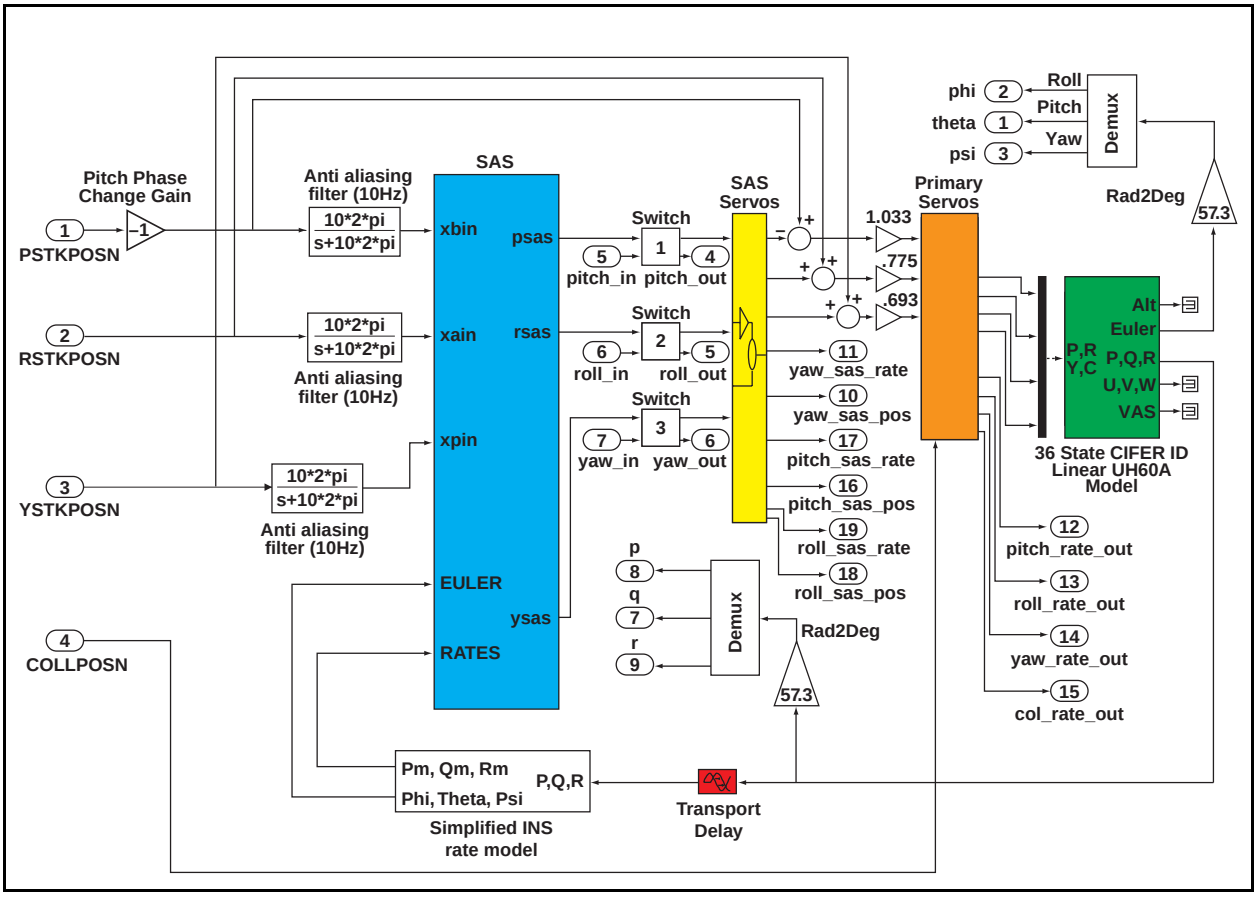

Figure 5. MCLAWS-2 ACAH Simulink¤ Block Diagram.

An accurate representation of the actuator dynamics is also of key importance to overall accuracy of the analysis. Previous studies used CIFER® to extract an accurate 2nd order transfer-function model of the actuator dynamic response from flight test data. The model was implemented in state-space form and included actuator rate and position saturation limits.

DETERMINATION OF DISCREPANCIES IN SIMULINK® ANALYSIS MODEL

Initial flight tests of the baseline gain set showed significant qualitative discrepancies with the predicted characteristics based on the Simulink® analysis model. An immediate project decision was made to conduct ground and flight tests to establish the source of these discrepancies and achieve a reliable "anchor point" for further design optimization using CONDUIT®. The tests and analysis were completed in a one-week focused effort that is illustrated in the following paragraphs.

Frequency-sweeps in pitch, roll, and yaw were conducted for the MCLAWS-2 baseline gain set at the hover flight condition in one hour of flight time. Standard frequency-sweep test techniques were used (Ref. 13), with maximum input amplitudes and frequencies kept within a range that avoided limiting of the SAS actuators (i.e., less than ±10% stick input). Example flight data for a roll sweep are shown in Fig 6. Three repeat roll sweeps were flown and concatenated in CIFER® for improved identification accuracy. The initial comparison of the system identification results with the Simulink® model verified that some significant mismatches in the gain and phase responses and were the likely cause of the observed qualitative discrepancies.

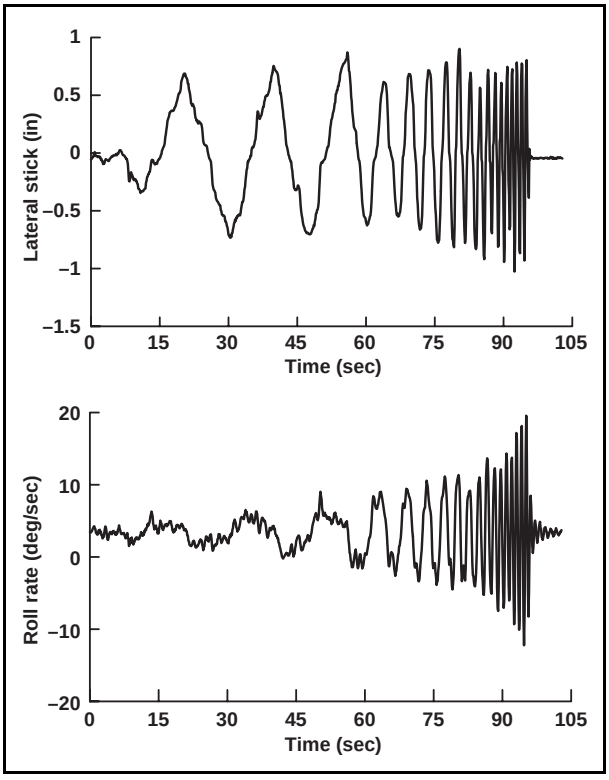

Figure 6. Flight test data for roll frequency-sweep.

The simplified roll-axis schematic of Fig. 7 illustrates the flight test measurements available. As can be seen, many of the internal Flight Control Computer (FCC) signals were recorded in the flight tests—a result of careful pre-flight planning. This allowed frequency-response identification of the key elements of the block diagram, which proved invaluable for isolating the various modeling discrepancies. Phase errors were observed in elements that should have been easily and accurately modeled, such as the command model and SAS actuator response. Some quick, but insightful, bench tests were conducted on the measurement system which exposed timing skews of up to 44 msec between the various measurement signals as the source of the observed phase errors. These skews were artifacts of the *measurement system itself*, and were not present in the MCLAWS-2 feedback quantities. The effects of these timing skews were corrected in the identification results, thereby allowing a valid comparison of the measured responses with the Simulink® model and an isolation of the remaining errors.

A second source of discrepancy between the analysis model and the flight tests was in the definition of cockpit stick deflection. The MCLAWS-2 control law implementation in the EH-60L incorporated units of stick deflection based on the idealized definitions of

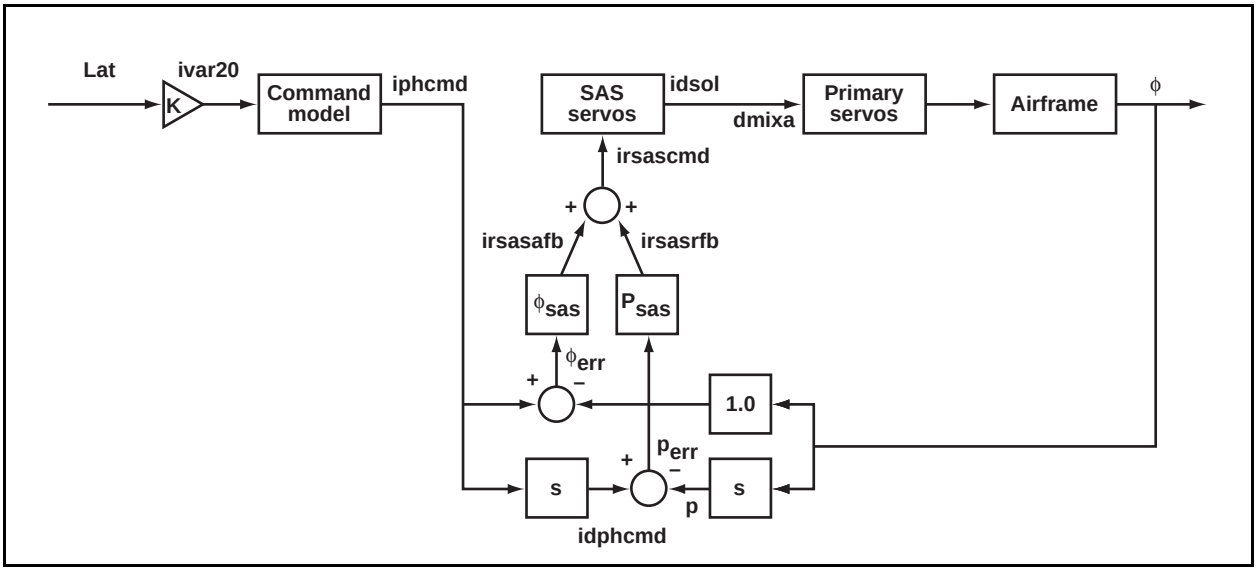

Figure 7. Simplified schematic of roll axis MCLAWS-2 implementation; measured parameters are indicated next to signal arrows.

stick throw and stick-to-mixer gearing as obtained from the GENHEL simulation (Ref. 14). The CIFER®-identified model used in the Simulink® analysis was based on direct measurement of true stick inches and carefully calibrated gearing as determined from ground-based measurements taken in the UH-60 helicopter. The inconsistent definition of stick deflection units resulted in fairly sizeable magnitude shifts (i.e., scale factor error) in the EH-60L bare-airframe response as compared to the identified model. Several additional discrepancies between the Simulink® modeling and aircraft implementation of the MCLAWS-2 control laws were also found and corrected.

The frequency-response of the corrected Simulink® block elements of Fig. 7 were determined using CONDUIT® and were rechecked against the flight data. Excellent agreement in all the axes was found both for the individual block elements as well as for the overall broken-loop and closed-loop responses. Some examples for the roll axis follow.

The roll command model ("command model" of Fig. 7) is identified from the transfer function:

$$P_{com} = (\text{iphcmd})/(\text{ivar20}) \qquad (2)$$

and is compared with the CONDUIT® model in Fig. 8. The coherence is nearly unity, indicating excellent accuracy as would be expected for identifying software elements as compared to airframe dynamics. The roll rate SAS dynamics (P_{sas} of Fig. 7) are identified (P_{sas} = irsasrfb/p_{err}) and again match the CONDUIT® model precisely as shown in Fig. 9. The dynamics of bare airframe response to mixer, p/dmixa, are seen in Fig. 10 to match the identified state-space model used in the CONDUIT® analysis (in the frequency range of good coherence), once the scale factor corrections discussed above are included. The broken feedback loop response, critical for determining crossover frequency and stability margins, is obtained by multiplying the individual identified responses using the frequency-response arithmetic function in CIFER®:

$$\text{broken loop} = [sP_{sas} + \phi_{sas}][(\text{p/dmixa})1/s](\text{sas servo}) \quad (3)$$

making direct use of the frequency-response data, for example P_{sas} of Fig. 9 and p/dmixa of Fig. 10. The broken-loop response for roll shows very good agreement with the analysis model as seen in Fig. 11. This ensures that the key control system metrics of crossover frequency, gain margin, and phase margin will be well predicted. Finally, the overall closed-loop response of p/Lat shows good agreement, as can be seen in Fig. 12, thereby ensuring that the handling-qualities parameters (bandwidth and phase delay) will be well predicted.

A summary of the broken-loop and closed-loop response metrics for the roll loop is presented in Table 2 for the baseline MCLAWS-2 gain set. The CONDUIT® predictions are generally seen to match the flight data quite well, as is expected from the good agreement in the frequency responses shown above.

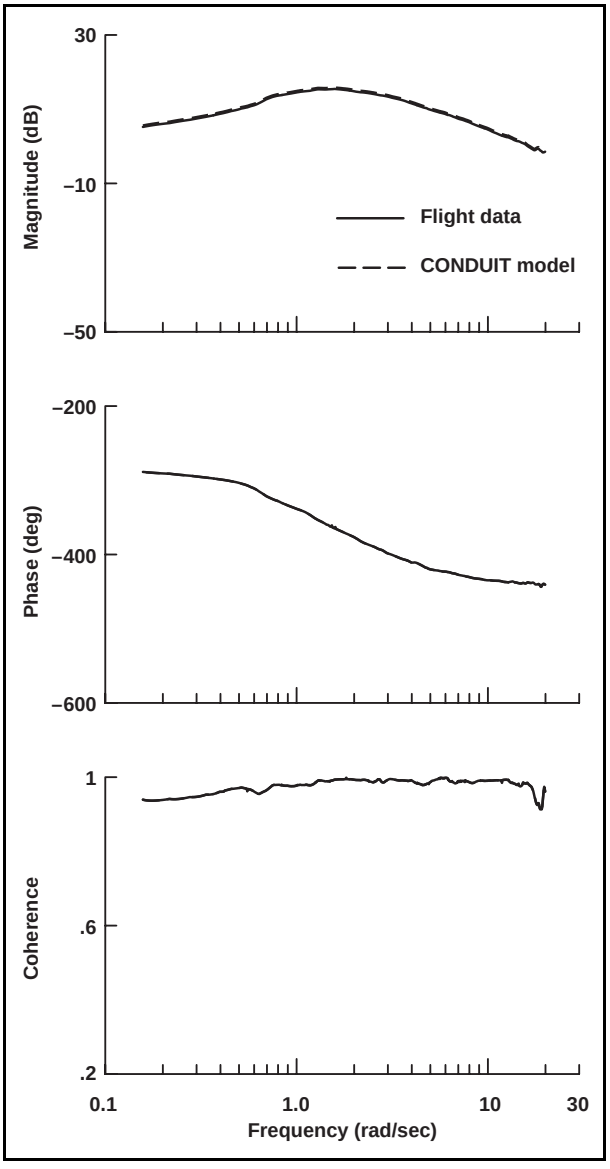

Figure 8. Command model comparison, roll axis.

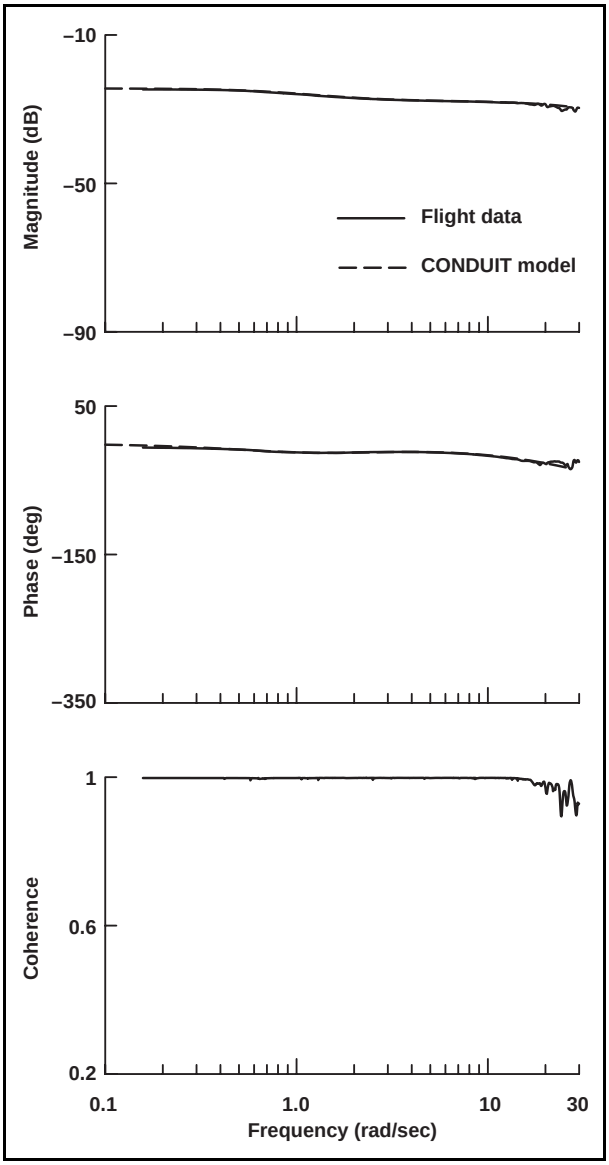

Figure 9. Roll rate SAS compensation comparison, P_{sas}.

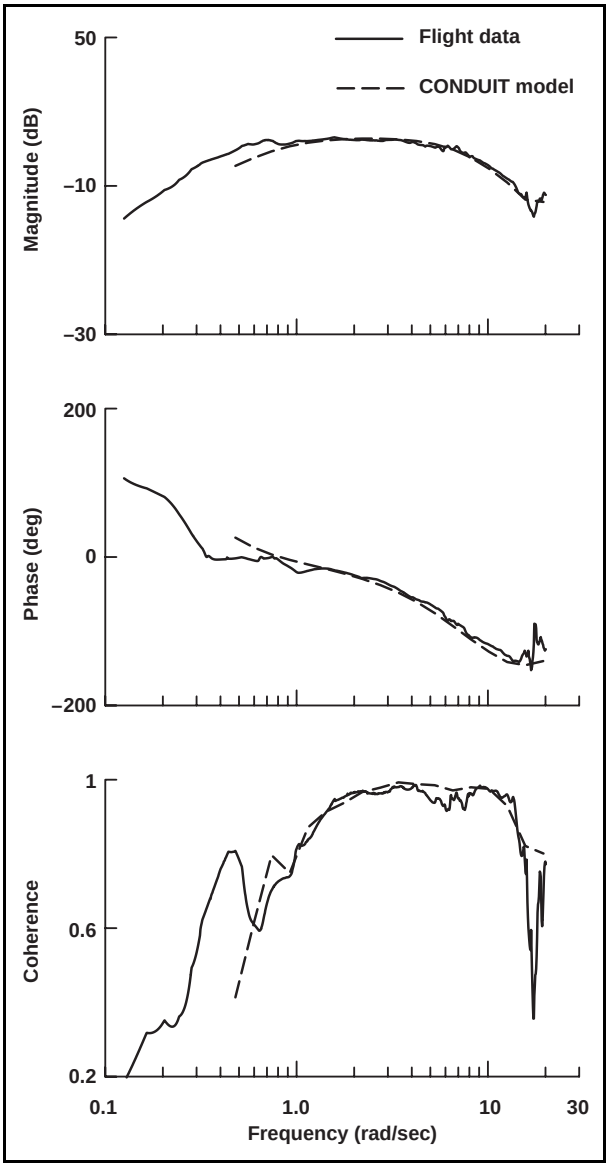

Figure 10. Bare airframe roll response comparison, p/dmixa.

The same level of agreement was achieved for the pitch and yaw channels. This analysis established that the updated CONDUIT® model provided a satisfactory anchor point (MCLAWS-2 baseline) from which design optimization was conducted.

CONDUIT® BASELINE ANALYSIS

Eight unique types of specification (or spec) listed in Table 3 were selected for the baseline analysis. Some specs were chosen to assess response versus ADS-33 handling qualities and MIL-F-9490D stability requirements, while others were Ames-derived and selected to address performance issues. The eigenvalues spec verifies that the closed-loop system is stable.

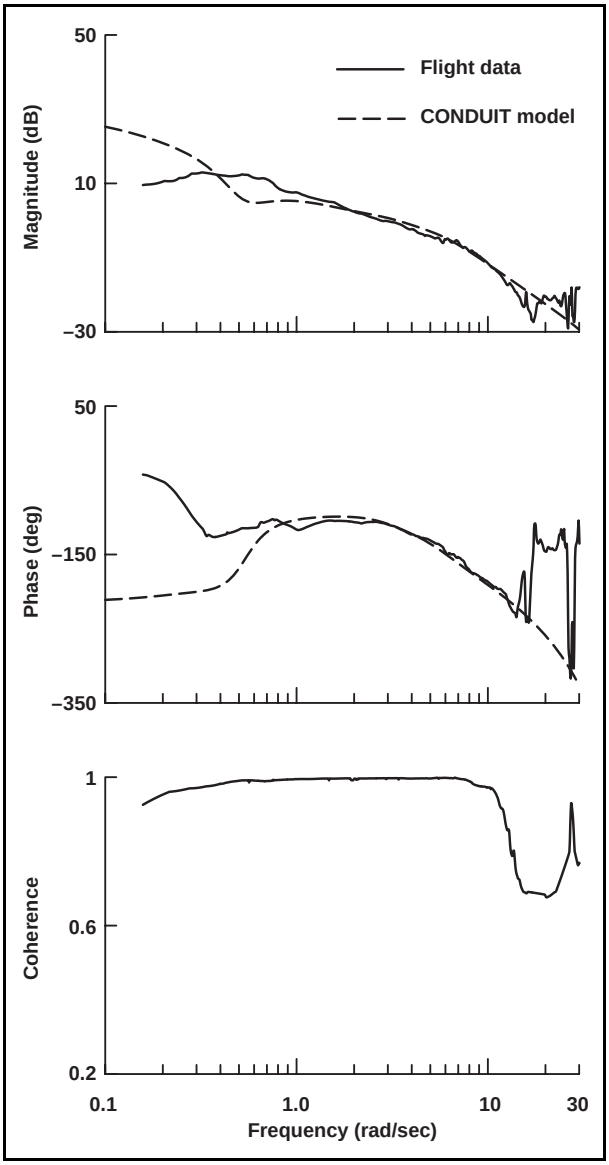

Figure 11. Roll broken-loop response comparison, Eq. 3.

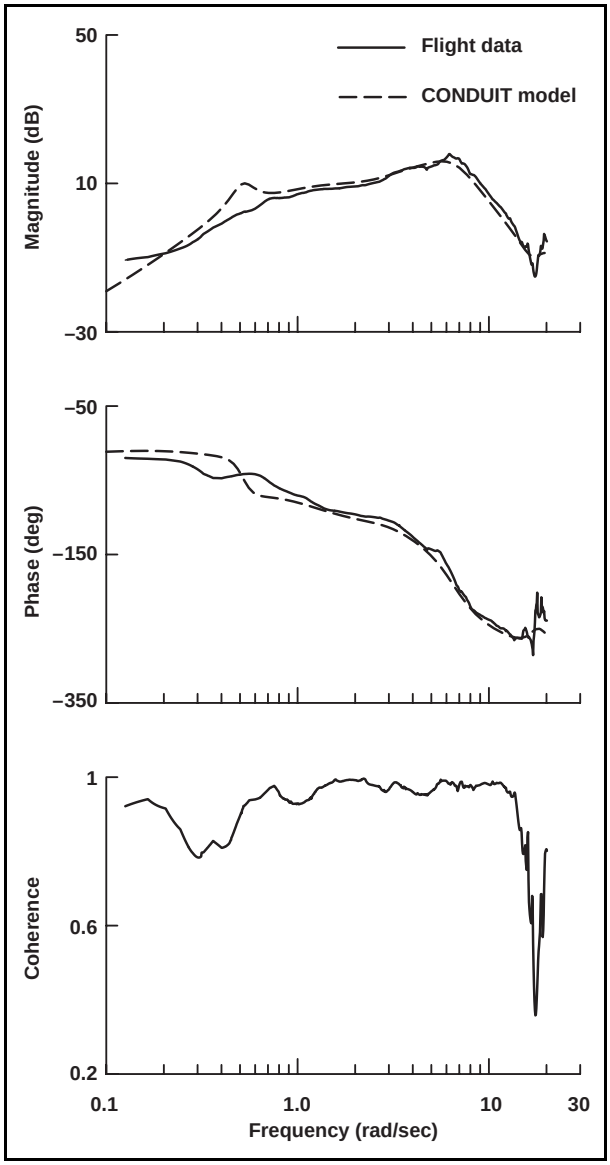

Figure 12. Roll closed-loop response comparison, p/Lat.

Table 2. Roll broken loop and closed loop response metrics for baseline gain set.

	ω_c, rad/sec	PM, deg	GM, dB	ω_{180}, rad/sec	BW, rad/sec	Phase Delay, sec
CONDUIT®	3.29	65.0	9.87	8.66	2.68	0.0762
Flight	2.74	73.0	9.68	9.05	2.03	0.0766

The stability margin spec verifies that satisfactory gain and phase margins are achieved for the broken-loop responses. In the yaw axis, the evaluation is completed for both: rate and attitude feedback (feet off pedals) and rate feedback only (feet on pedals). The bandwidth specs are key short-term response requirements in ADS-33, and are directly related to the step-response rise time. The damping ratio spec determines the damping ratio of all closed-loop complex poles to verify that the system is well damped. The crossover frequency and the actuator root mean squared (RMS) specs were included for use in the control system optimization (discussed later) and drive the design to achieve the specifications with minimum overdesign. Finally, the frequency-domain pitch/roll coupling spec was included to track the influence of the feedback system on response cross coupling. Considering the three control axes, a total of 12 specs were used in the baseline analysis.

An evaluation was first conducted on the MCLAWS-2 baseline configuration, which was the initial gain set based on linear analysis and extensive non-linear piloted simulation. The evaluation results are shown in Fig. 13 in the form of the CONDUIT® Handling-Quality (HQ) window. The dark gray region in each spec represents Level 3 handling qualities ("deficiencies require improvement"), the light gray region represents Level 2 ("deficiencies warrant improvement"), and the white region represents Level 1 ("satisfactory without improvement").

As can be seen from Fig. 13, the roll axis for the baseline design predicts overall satisfactory handling qualities and control system performance, with all specs meeting the Level 1 requirements. The yaw characteristics are also satisfactory, except for yaw bandwidth (BnwAtH1), which achieves only Level 3 handling qualities. Finally, the pitch axis displays a Level 3 stability margin (StbMgG1) and Level 2 bandwidth (BnwAtH1), the later resulting from a very low crossover frequency (CrsLnG1). The pitch-roll coupling is unchanged from the standard EH-60L and results both from the inherent coupling of all rotorcraft as well as the influence of the canted tail-rotor. Crossfeeds were developed in analysis and found to be effective in reducing pitch-roll coupling, but were not evaluated during the limited flight program.

It is important to note that the same baseline handling-qualities evaluation discussed in this section was originally conducted on the uncorrected simulation model, prior to the determination and resolution of model discrepancies. These original results showed better (and thus misleading) performance in general. This finding underlies the importance of having an well validated aircraft model to minimize flight test time and achieve improved handling qualities in a rational and predictable manner.

Table 3. CONDUIT® specs for UH-60 analysis.

Requirements	Source	Spec Name	Channel	Constraint Type
Eigenvalues	Ames	EigLcG1	—	Hard
Stability margins	MIL-F-9490D	StbMgG1	Pitch, roll, and yaw	Hard
Bandwidth	ADS-33	BnwAtH1	Pitch and roll	Soft
Damping ratio	Ames	EigDpG1	—	Soft
Crossover frequency	Ames	CrsLnG1	Pitch	Objective
Actuator RMS	Ames	RMSAcG1	Pitch	Objective
Bandwidth	ADS-33	BnwAtH1	Yaw-rate feedback	Check only
Pitch and roll coupling	ADS-33	CouPRH2	Pitch/roll	Check only

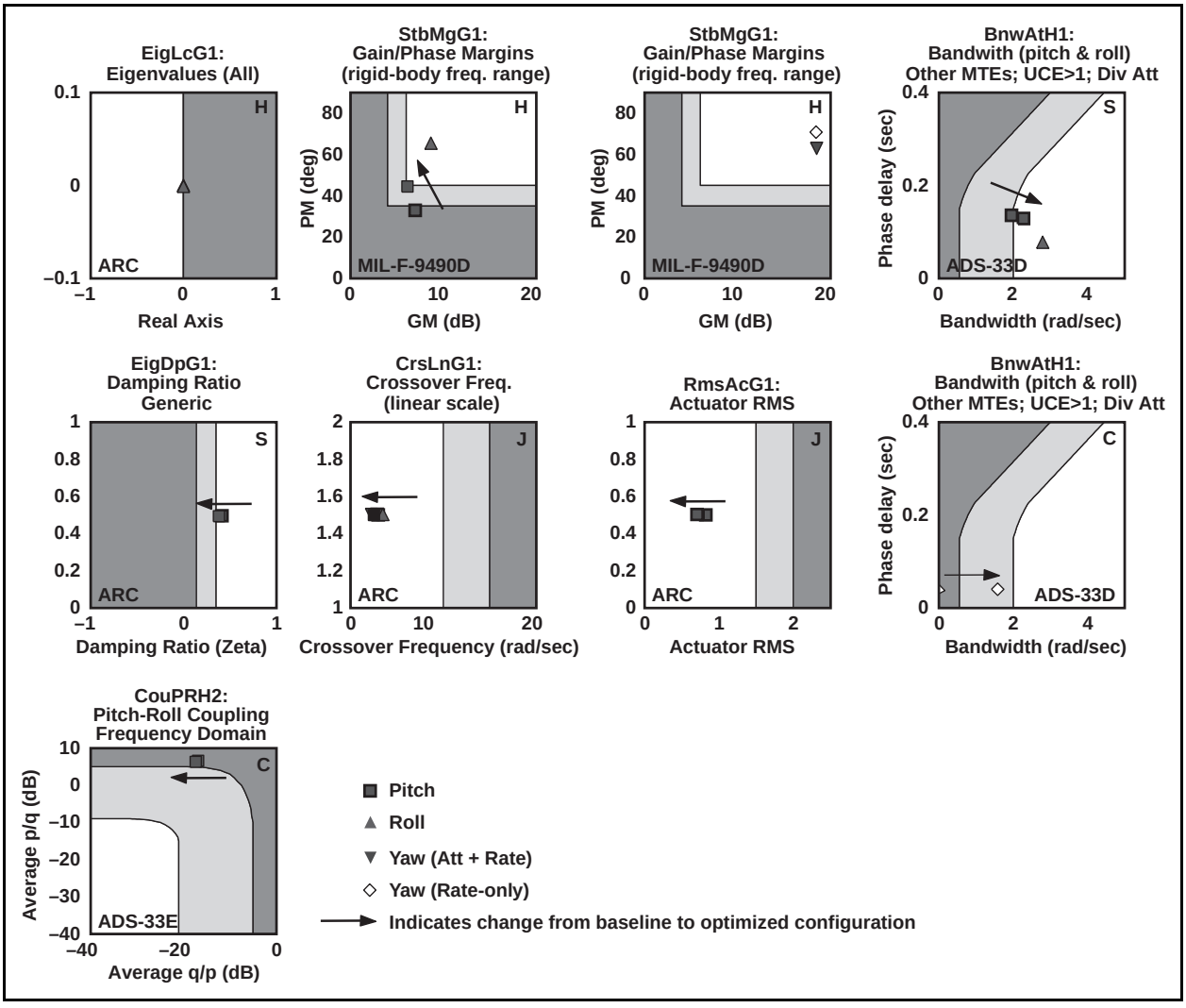

Figure 13. CONDUIT® handling-qualities evaluation for the baseline and optimized baseline (DM = 0%) configurations.

A preliminary flight test evaluation was conducted for the MCLAWS-2 baseline gain set to provide some initial pilot comments. Key comments related to handling-qualities issues were:

- "No residual roll oscillations following lateral pulse."
- "No cross coupling following the longitudinal pulse."
- "Configuration was stable with the exception of a 1-2 cycles of roll oscillation after achieving a stabilized hover."
- "Very nice attitude command response during the maneuver."
- "Three to four cycles of roll oscillations occurred following the feet-off the micro-switches pedal input."
- "Maneuver performed within desired tolerances, but longitudinal drift resulted in some excursions into adequate."
- "Longitudinal and lateral drift more pronounced."

These pilot comments generally track the CONDUIT® baseline evaluation results well. A consensus was reached that emphasis for design improvement was needed on the pitch channel command and disturbance response, and the yaw channel bandwidth. The roll channel response was judged to be satisfactory without improvement.

CONDUIT® OPTIMIZATION

The yaw bandwidth deficiency was easily resolved using CONDUIT® in a manual mode. The command model frequency was increased from 2.0 rad/sec to 3.3 rad/sec, which brought the response to near Level 1 compliance. Further, increases in command model frequency resulted in excessive SAS actuator limiting. The remaining efforts in control law optimization focused on addressing the pitch axis deficiencies only. The same specs used in the baseline evaluation were used for this optimization study.

For control law optimization in CONDUIT®, the user declares each of the specifications to belong to one of the following five classes: hard constraint, soft constraint, performance objective criterion, summed objectives, or check-only (Ref. 15). The selection of specification class defines the solution strategy for the optimization process. For the pitch design optimization, the choice of constraint type for each spec is listed in Table 3. In the pitch axis MCLAWS-2 block diagram, six gains were defined as design parameters to be tuned in CONDUIT®. These gains are listed in Table 4.

Optimization is conducted in three distinct phases. In *Phase 1*, the design parameters are tuned to ensure that the hard constraints are satisfied. Once all the hard constraints meet the Level 1 criteria, the optimization process moves into *Phase 2* and begins to work on the soft constraints. When the design satisfies all the Level 1 requirements for the soft constraints, a feasible (but not optimal) design solution is reached, and the optimization process enters *Phase 3*. In Phase 3, CONDUIT® will tune the design parameters to optimize the system based on the selected performance criteria while ensuring that the Level 1 requirements are still met. In the MCLAWS-2 optimization study, the pitch crossover frequency and the actuator RMS specs were defined as the objective functions to minimize the actuator demands to pilot and turbulence inputs. This strategy ensures minimum overdesign relative to the Level 1 boundaries. Further detailed discussion on the CONDUIT® optimization process can be found in Reference 15.

The optimized baseline feedback gains to meet the minimum Level 1 requirements are listed in Table 4 ("0% DM"). Significant changes relative to the baseline (60-70%) are seen in the integral and attitude gains. Also, a lead-lag compensation with two tunable time constants was introduced to provide the added phase lead needed to achieve the required stability margins. The remaining gains are modified to less than 10%. The handling-qualities prediction of the optimized system is shown in Fig. 13 for comparison with the baseline system. The arrow in each sub-figure shows the direction of change from the baseline to the optimized system. As can be seen, all pitch characteristic now meet the Level 1 requirements. The yaw response bandwidth is now nearly Level 1 as discussed earlier, and the roll response is unchanged from the baseline. These results showed the need for significant modifications to the control system configuration and gain set as obtained from the piloted simulation. This has been a common theme in the development of advanced control systems for rotorcraft (Refs. 16, 17). Direct control system optimization in CONDUIT® using a validated math model and relevant design requirements assured that flight evaluation could proceed with a minimum of costly tuning.

Table 4. Relative comparison of final pitch gain sets for the four configurations.

	Baseline	Optimized Baseline (0% DM)	8% DM	10% DM
Pitch SAS feedback gains				
Attitude integral gain	1.00	1.71	1.59	1.81
Attitude gain	1.00	0.58	0.47	0.38
Rate lag filter time constant	1.00	1.00	1.11	1.03
Lead/lag compensator lag time constant	1.00	0.97	0.94	0.81
Lead/lag compensator lead time constant	1.00	1.09	1.30	1.20
Rate lag filter gain	1.00	1.00	1.05	1.12

The specifications, such as ADS-33 and MIL-F-9490D, that form the key design requirements for CONDUIT® provide for the *minimum response characteristics* to just achieve Level 1 ("satisfactory without improvement"). As the response is driven more deeply into the Level 1 region, faster response, better disturbance rejection, and improved margin for uncertainties are all achieved, providing for improved handling qualities. The cost for this is increased actuator usage and reduced stability margins. At some point, further increases into the Level 1 region cannot be achieved without: (1) degradation of stability/damping into the Level 2 region, or (2) excessive actuator usage/saturation.

A design margin (denoted DM) is defined in CONDUIT® as the fractional increase in the desired Level 1 boundary relative to the actual mil-spec criteria. As shown in Fig. 14, the design margin is defined in terms of a fraction of the width between the Level 1 and Level 2 boundaries. In this example, a 10% design margin sets the acceptable Level 1 design boundary to a position that is inside the actual ADS-33 Level 1 by a distance that is 10% of the width of the Level 2 region. So, the nominal design to just meet ADS-33 is associated with DM = 0%. The Design Margin Optimization feature in CONDUIT® automatically re-tunes the control system for an increasing value of design margin applied uniformly to all design specs. This results in a *family of optimized solutions* based on uniformly increasing performance into the Level 1 region. As the design margin is increased, the optimization engine attempts to drive all the constraint specs further into the Level 1 region, until one or more specs fails to achieve the more stringent criteria. The final design is selected by the users from an assessment of the tradeoff between performance improvement and actuator usage as embodied in the family of solutions obtained by CONDUIT®.

Fig. 15 illustrates the typical tradeoff behavior for a range of design margin values. Note that units for the y-axis of this Figure are in terms of the "Pcomb." As discussed in more detail in Reference 18, the "Pcomb" or "Performance Comb" is a normalized value of the numerical rating of the design point on each spec in CONDUIT®. A value of Pcomb = 1 indicates that the design point lies on the Level 1 boundary, and a value Pcomb <1 indicates how far the design point is into the Level 1 region. So, a lower value of Pcomb indicates improved performance. As mentioned in the example earlier, a 10% design margin sets the Level 1/Level 2 boundary 10% of the width of the Level 2 region into the Level 1 region of a spec. The new boundary is now the "effective" Level 1/Level 2 boundary of the spec. Thus, a Pcomb value of 0.9 now indicates that the design point lies on the Level 1/Level 2 boundary for the 10% design margin case.

As illustrated in Fig. 15, a control system is initially designed and optimized to just meet ADS-33 with 0% design margin. As the design margin increases, which implies that the Level 1 region of all the specs is smaller, better overall performance (faster response, improved agility, better stability, for instance) can be achieved at the expense of increased control activity (leading to saturation) and degraded stability margins. Eventually, as shown in the figure, the control activity (and stability) specs intersect the effective Level 1/ Level 2 boundary, and no further increase in design margin is possible. The MCLAWS-2 design was

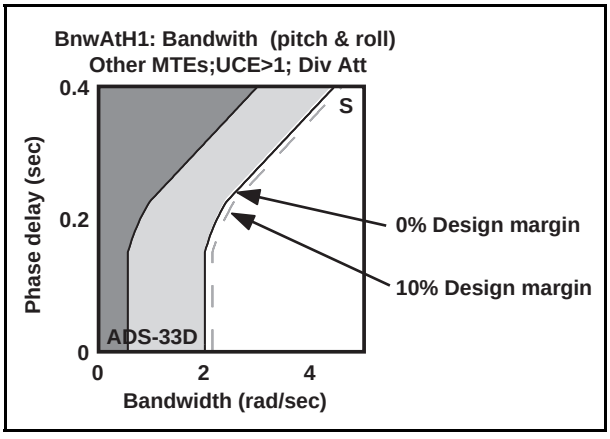

Figure 14. Example of design margin.

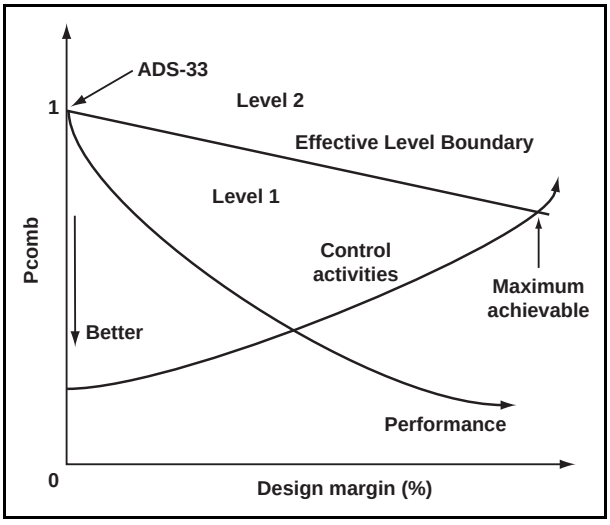

Figure 15. Concept of design margin optimization.

optimized for increasing values of design margin (DM) using the CONDUIT® design margin optimization feature. Fig. 16a-16e show the effect of increasing design margin on the various pitch specs, in terms of the Pcomb values.

As the design margin is increased, both the pitch stability margin (Fig. 16a) and bandwidth (Fig. 16b) specs are driven further into Level 1, which implies better stability and responsiveness. The increase in bandwidth is achieved by an increase in the crossover frequency as can be seen in Fig. 16c. The increased bandwidth also increases frequency and amplitude of the pitch actuator demands as expected (Fig. 16d). Eventually the drive for increased crossover frequency causes the pitch stability margin and closed-loop damping ratio to be reduced to where they cross over the Level 1 boundary and enter the Level 2 region. The pitch damping ratio now cannot achieve Level 1 performance for the 10% design margin (circle symbol in Fig. 16e). Further increases in design margin are not achievable, so the optimization stops at this point. Recall that originally, the damping ratio performance was solidly in the Level 1 region for the DM = 0% design. Such behavior confirmed the expected tradeoff trends discussed earlier.

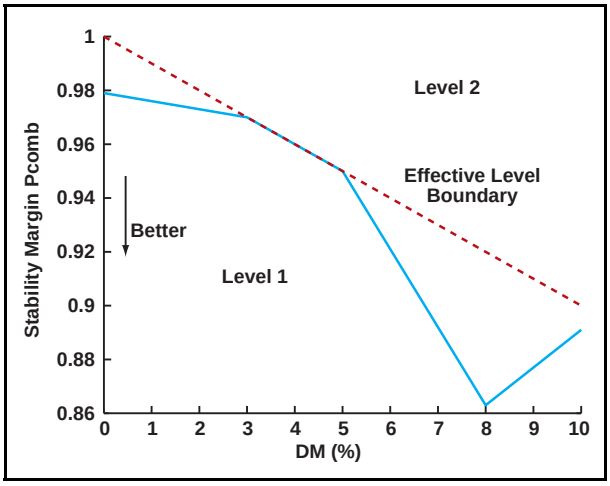

(e)

Figure 16. Design margin optimization.

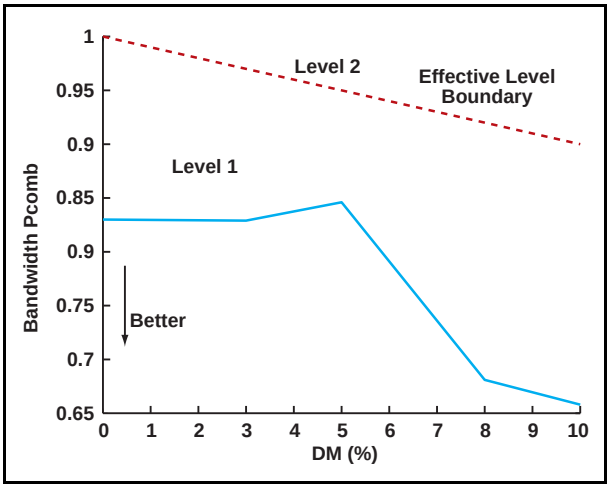

(b)

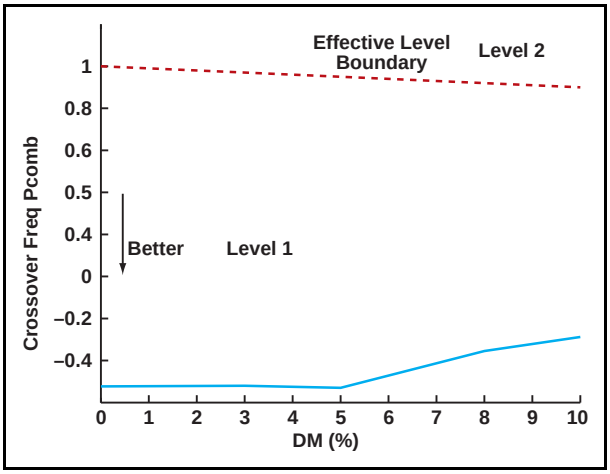

(c)

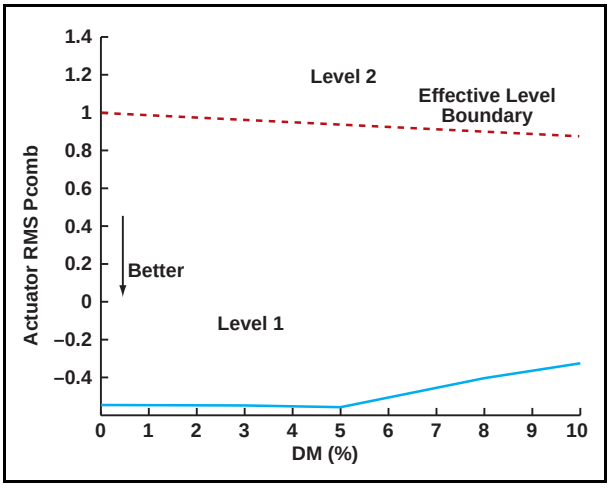

(d)

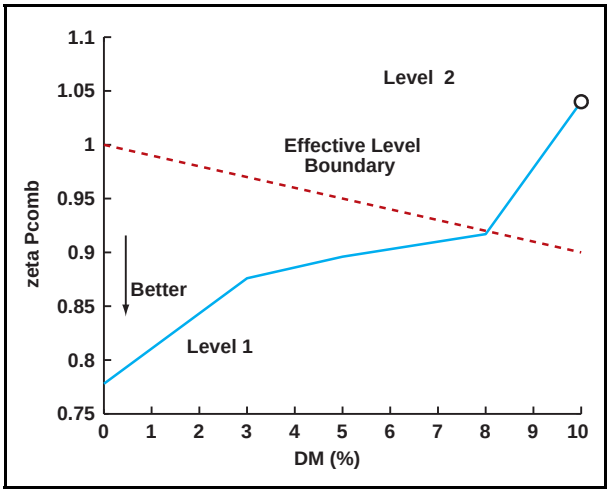

(e)

Figure 16. Design margin optimization (concluded).

Fig. 17 shows the overlay of HQ windows for DM = 0%, 8%, and 10%. The effect of increasing design margin is indicated by the gray arrows, and reflects the performance trends of Fig. 16a-e. Table 4 shows the comparison of the gain sets of these three configurations relative to the normalized baseline set.

From this study, it can be concluded that the 8% DM case is the optimum case, with all the specs meeting Level 1 criteria and significant improvements in handling qualities and performance, while maintaining reasonable demands on actuator activity. The 10% DM case yields improvement in the design responsiveness, but with a less well damped response to disturbances. As discussed later, flight tests were conducted to evaluate the handling-qualities tradeoff between the 8% and 10% DM design, and the pilots' consensus was preference for the 10% DM case. The 10% DM design was evaluated for robustness to uncertainties in the identified math model parameters, as discussed next.

Robustness Analysis for 10% Design Margin Case

The robustness of the DM =10% design was examined using the Robustness Analysis Tool in CONDUIT®. This tool analyzes the variation in predicted handling-qualities and performance with respect to parametric model uncertainties.

The full state-space CIFER® identified model for the UH-60 as described in Eq. (1) contains 61 identified physical parameters. These parameters have been propagated to 82 entries throughout the system matrices (M, F, G) in Eq. (1), as illustrated in Fig. 18. For each identified physical parameter, CIFER® provides both the nominal value and the associated statistical 1σ confidence bound as shown in Fig. 18. All of the analyses conducted in CONDUIT® described thus far were based on using the nominal values of the identified physical parameters as reflected in the matrices (M, F, G) in Eq. (1). The parametric model uncertainties considered in the present robustness analysis are based on the 1σ perturbation bounds of the identified physical parameters, not on direct independent perturbations of the elements of the matrices in Eq. 1. More specifically, the parametric model uncertain control system considered in this study can be described as:

$$\begin{aligned}(M+\Delta M)\dot{x} &= (F+\Delta F)x+(G+\Delta G)u \\ y &= Hx+Ju\end{aligned} \tag{4}$$

where M, F, G, H, and J are matrices of nominal values for the identified aircraft model, and all the parametric model uncertainties are contained in ΔM, ΔF, and ΔG matrices.

As shown in Fig. 18, it is important to note that there are identified physical parameters which appear in multiple entries in Eq. (1); such as the rotor flapping time constant τ_f which appears in both the M and F matrices. As a result, the 1σ perturbation to τ_f, say $\Delta\tau_f$, would also appear in both ΔM and ΔF matrices in Eq. (4). Moreover, as shown in Fig. 18, some entries in Eq. (1) could be constrained by one or multiple identified physical parameters; such as *param1* in the F matrix, and *param2* and *param1*param2* in the G matrix. In this case, the 1σ perturbations to *param1* and *param2*, say Δ*param1* and Δ*param2*, would propagate accordingly to the ΔF and ΔG matrices. So, for example, the perturbation term corresponding to "*param1*param2*" in the Δ*G* matrix is (*param1**Δ*param2* + *param2**Δ*param1* + Δ*param1** Δ*param2*).

The characterization of uncertainty for the state-space model is thus seen to be highly structured owing to the relationships between the identified physical parameters and the state-space model matrices. These same relationships define the structure of the uncertainties in the state-space matrices. Hence, the class of uncertain systems described in Eq. (4) is quite different from that commonly considered in the context of robust/ H^∞ control where the uncertainty is assumed to be unstructured and belong to some norm-bounded set. Furthermore, when the leading term "M+ΔM," which is invertible for all admissible ΔM, is inverted and multiplied through Eq. (4) to form the standard state-space representation, the resultant uncertain system description would be more complex (and the

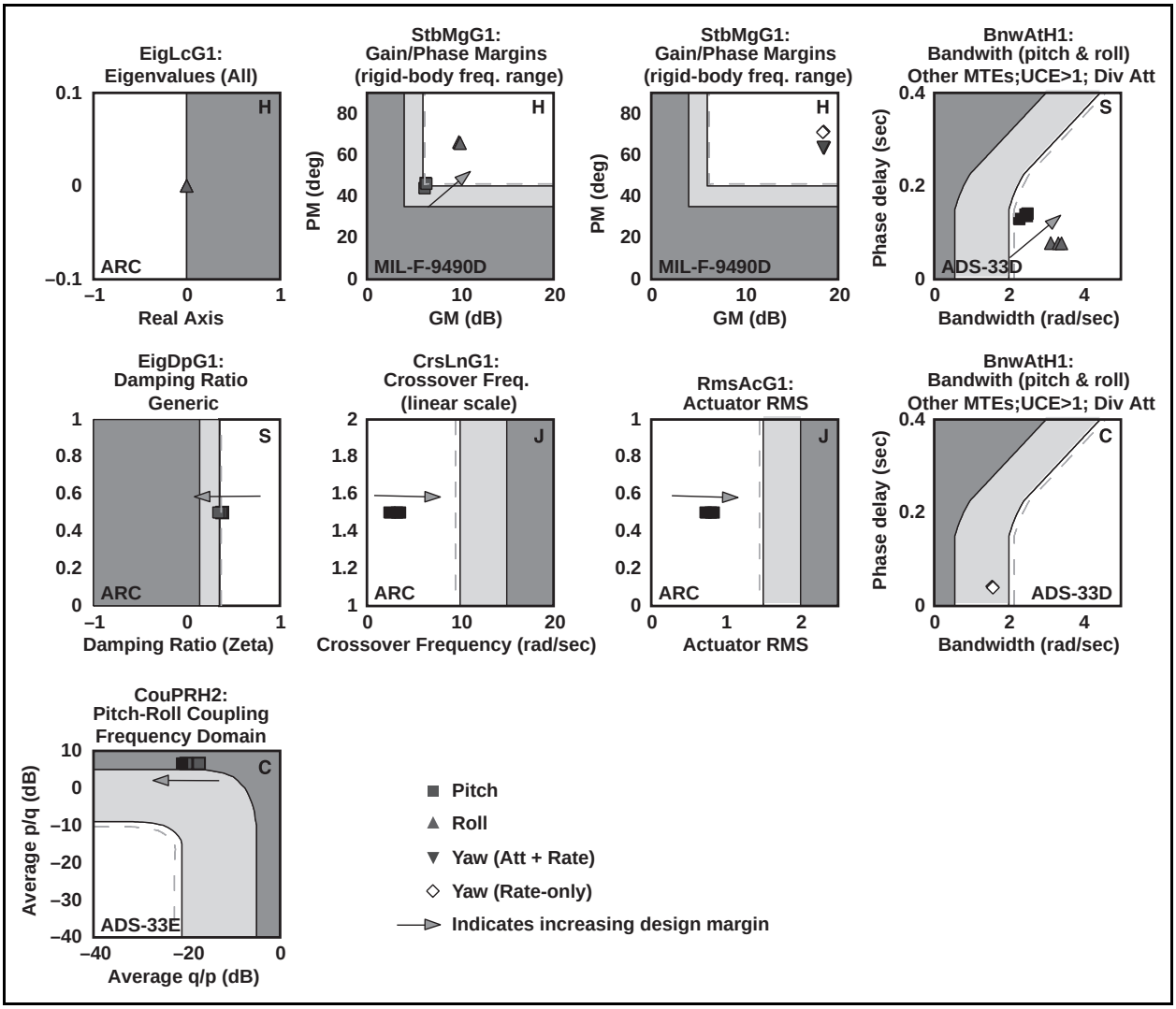

Figure 17. Handling-Qualities window overlay of DM = 0%, 8%, and 10%.

robustness of its control system more difficult) to analyze by using the conventional robust/ H^{∞} control approach. The CONDUIT® Robustness Analysis Tools, on the other hand, were developed to handle the uncertain control systems with structured parametric model uncertainties as described in Eq. (4). In the discussion that follows, we present the detailed robustness analysis procedure and results for the 10% DM design solution.

The CONDUIT®/CIFER® integration routines that are part of CONDUIT® allow direct extraction of the CIFER® identified aircraft model and associated 1σ perturbation bounds from the CIFER® database. A randomized set of cases are formed by first perturbing the actual identified parameters and propagating them throughout (ΔM, ΔF, ΔG) in Eq. (4). Each perturbed case is then converted to standard state-space form:

$$\begin{aligned} \dot{x} &= Ax + Bu \\ y &= Cx + Du \end{aligned} \tag{5}$$

for evaluation in CONDUIT®. A total of 30 perturbation cases were simulated in CONDUIT®. The perturbation increment for a particular identified parameter is randomly selected as the +1σ or -1σ value of the uncertainly bound for the parameter as given in Ref. 7. A single perturbation case is formed by simultaneously varying all of the identified physical parameters with the randomized value (+1σ or -1σ) as appropriate to each parameter, and then conducting the handling-qualities analysis.

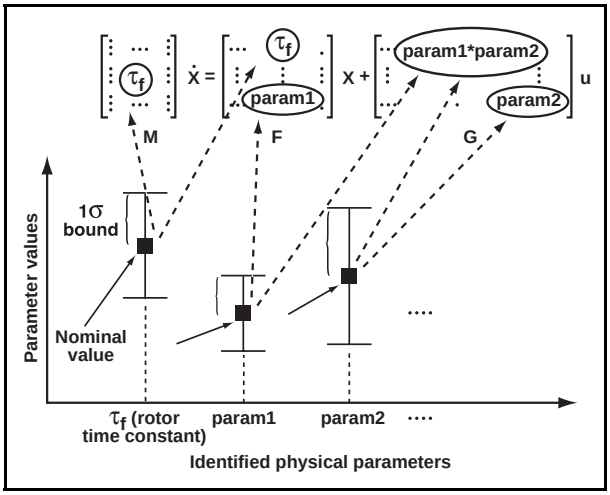

Figure 18. An illustrative example showing how CIFER$^{\alpha}$ identified physical parameters relate to the aircraft state space model.

The evaluation of the 30 perturbed cases are displayed along with the nominal case (i.e. no perturbation) in Fig. 19. The nominal case is highlighted (light color), while all other perturbed cases shown in the dark colored symbols. It can be seen in Fig. 19 that the performance of all of the perturbed cases remain fairly close to that of the nominal case. In most cases, the spec values remain in either the Level 1 or Level 2 region. The key exception is the eigenvalue spec (EigLcG1), which crosses into the Level 3 region, indicating instability for some perturbed cases. However, examination of these perturbed cases reveals that the instability was caused by some very low frequency unstable poles in the closed loop system (the fastest pole is at 0.05 rad/sec). While the strict interpretation of ADS-33 for attitude-response systems requires that all eigenvalue be stable, these very low frequency modes have time constants that are slow enough to be

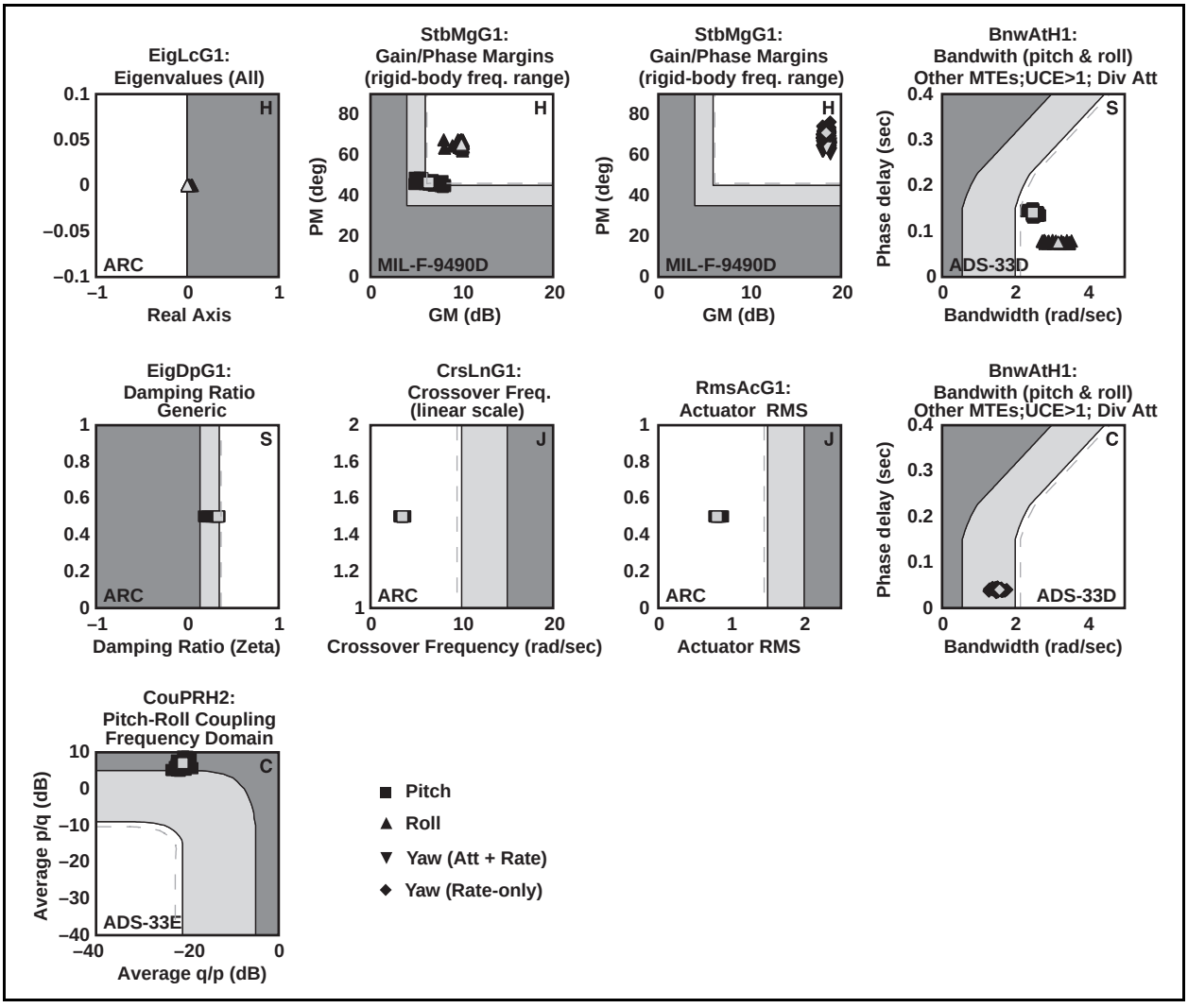

Figure 19. Robustness analysis of DM = 10%; light color symbol is nominal case.

inconsequential. Overall, it can be concluded that the 10% DM MCLAWS-2 configuration can be expected to be robust to uncertainties in the aerodynamic parameters.

FLIGHT TEST EVALUATION OF OPTIMIZATION CASES

Following CONDUIT® optimization, quick piloted assessments were obtained using the RIPTIDE real-time simulation capability (Fig. 4). The assessment provided the safety pilot with an important initial impression and a high degree of confidence prior to RFCC engagement. Flight assessments of the various MCLAWS-2 configurations were performed on the Army/NASA EH-60L aircraft. These flight evaluations focused on the baseline configuration, and the 8% and 10% DM cases. Initial assessments were made from control pulse inputs in each axis, but it was difficult to select an overall best configuration based on the single-axis inputs. To assess these configurations in a more multi-axis control task, the ADS-33 Hover maneuver was performed. The maneuver cueing and performance standards were the same as developed and used for Reference 19.

Pilot comments from the Hover maneuver with the 10% DM case show that the pilots were able to make a smooth deceleration into the hover position, and that maintaining a stabilized hover required a low pilot workload (minimal pilot input required). Pilot comments from the 8% DM case indicate that the aircraft open-loop response was very stable in all axes, but the aircraft was somewhat difficult to stabilize with the pilot in the loop. For the baseline configuration, the pilots commented that more workload was required to maintain desired performance standards due to lateral and longitudinal drift. In the end, a consensus was reached that the 10% DM configuration indeed yielded the best overall performance.

To assess the 10% DM configuration in a broader evaluation, the 10% DM configuration and the EH-60L standard SAS/FPS configuration were evaluated while performing the ADS-33 Hover, Vertical, Lateral Reposition, and Departure/Abort maneuvers. In addition, a Sikorsky-developed maneuver, called an aggressive approach to hover, was also evaluated.

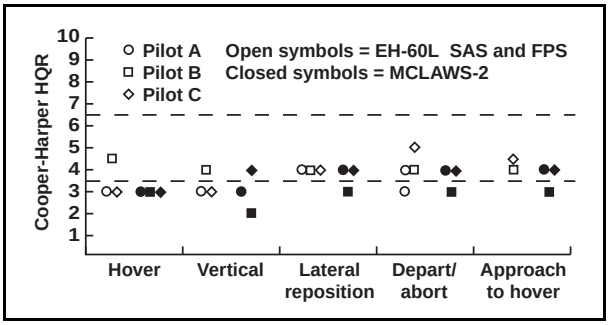

Figure 20. Handling-quality evaluations of MCLAWS-2 and the EH-60L standard SAS/FPS.

Fig. 20 shows the Cooper-Harper handling quality ratings (Ref. 20) for the five maneuvers from three pilots. The results show a consistent but small improvement with MCLAWS-2 compared to the EH-60L standard SAS/FPS configuration. However, it must be remembered that this comparison was conducted on a calm, clear day, and the primary advantage or benefit of the attitude command control laws is realized in the degraded visual environment. In contrast, there have been suggestions that the added stability of an attitude command response type can appear sluggish to the pilot in the day (good visual environment).

From the pilot evaluations (Fig. 20) and associated comments, it appears that the MCLAWS-2 attitude command response type does not appear to be sluggish or degraded compared to the EH-60L rate command response. In fact, pilot comments indicate that compared to the EH-60L standard SAS/FPS configuration, the 10% DM MCLAWS-2 configuration has less control activity, is more predictable, requires less pilot workload, and overall, showed significant benefits. To help illustrate this, Fig. 21 shows a sample time history for the standard EH-60L and 10% DM case from performing the ADS-33 Hover maneuver. Note that with the 10% DM case, hands-off performance was possible in low wind conditions for durations of three-to-four seconds following the deceleration.

The next phase of this work will be to incorporate the trim servos (MCLAWS-1) (Ref. 21) and explore the feasibility of performing the handling quality evaluations in the degraded visual environment.

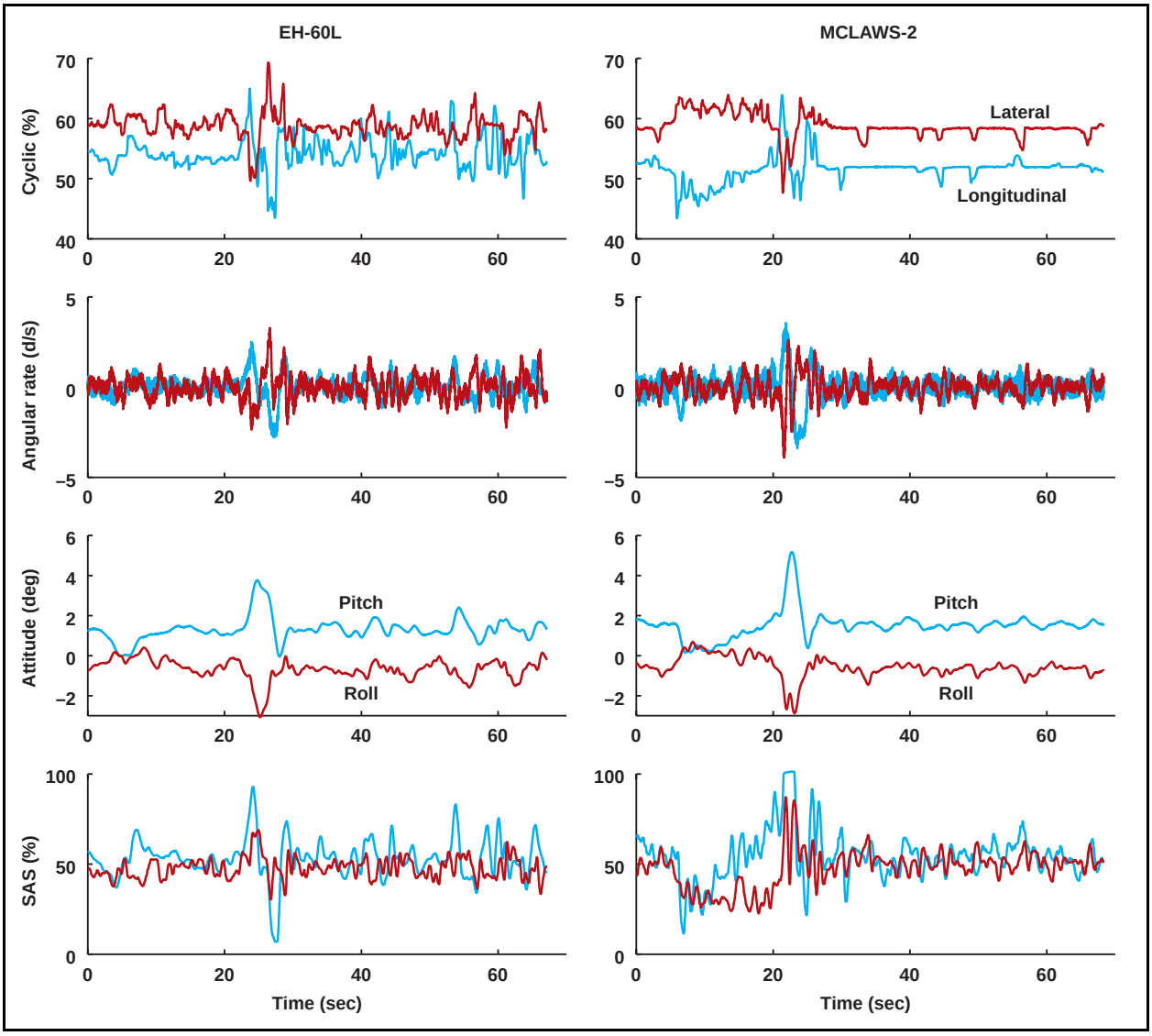

Figure 21. Comparison of standard Black Hawk SAS/FPS control laws versus the MCLAW-2 optimized control laws for the ADS-33 hover maneuver.

CONCLUSIONS

An initial set of modern control laws (MCLAWS-2) was developed for and evaluated on an EH-60L helicopter in a rapidly executed program. Central to addressing the significant resource and technical challenges of this project was the extensive use of a modern integrated toolset, comprised of block diagram simulation (Simulink®), system identification (CIFER®), control system analysis and optimization (CONDUIT®), real-time rapid prototyping (RIPTIDE), and pictures-to-code conversion.

The key findings were:

1. A short, focused program of ground test and frequency-sweep flight tests (one hour of flight data) of the MCLAWS-2 baseline gain set allowed the comprehensive validation and updating of the math model to be completed using system identification methods. This provided a validated “anchor point” as the basis for reliable control system optimization.
2. Control system optimization to meet the desired handling-qualities criteria for the validated analysis model resulted in significant

modifications to the baseline configuration as obtained from the piloted simulation.

3. A family of optimized designs was determined for increasing values of design margin, thus achieving a uniform increase in predicted performance relative to the ADS-33 minimum requirements. The optimized design (with 10% design margin) was shown to be robust to uncertainty in the identified physical parameters.

4. A flight test evaluation by three test pilots showed significant benefits of the MCLAWS-2 attitude-response type system with an optimized gain set (10% DM) compared to the EH-60L standard SAS/FPS system.

REFERENCES

1. "Aeronautical Design Standard, Handling Qualities Requirements for Military Rotorcraft," ADS-33E-PRF (USAAMCOM), 2000.

2. Sahasrabudhe, V, et al, "Piloted Evaluation of Modernized Limited Authority Control Laws in the NASA-Ames Vertical Motion Simulator (VMS)," American Helicopter Society 59th Annual Forum Proceedings, Phoenix, AZ, 6-8 May, 2003.

3. "Using Simulink®," The MathWorks Inc., November 2000.

4. Tischler, M. B. and Cauffman, M. G., "Frequency-Response Method for Rotorcraft System Identification: Flight Applications to BO-105 Coupled Rotor/Fuselage Dynamics," Journal of the American Helicopter Society, Vol. 37, No. 3, pp. 3-17, July 1992.

5. "CONDUIT® Version 4.1 User's Guide," Raytheon ITSS 41-071403, July 2003.

6. Mansur, M., Frye, M., and Montegut, M., "Rapid Prototyping and Evaluation of Control Systems Designs for Manned and Unmanned Applications," American Helicopter Society 56th Annual Forum Proceedings, Virginia Beach, VA, May 2000.

7. Fletcher, J. W. and Tischler, M. B., "Improving Helicopter Flight Mechanics Models with Laser Measurements of Flapping," American Helicopter Society 53rd Annual Forum Proceedings, Virginia Beach, VA, 29 April-1 May, 1997.

8. "Real-Time Workshop User's Guide," The MathWorks Inc., November 2000.

9. Tischler, M. B., "System Identification Requirements for High-Bandwidth Rotorcraft Flight Control System Design," AIAA Journal of Guidance, Control, and Dynamics, Vol. 13, No. 5, pp. 835-841, 1990.

10. Frost, C. R., Hindson, W.S., Moralez, E., Tucker, G., and Dryfoos, J. B., "Design and Testing of Flight Control Laws on the RASCAL Research Helicopter", Proceedings of the American Institute of Aeronautics and Astronautics Modeling and Simulation Technologies Conference, Monterey, CA, August 2002.

11. Lusardi, J., Blanken, C., and Tischler, M. B., "Piloted Evaluation of a UH-60 Mixer Equivalent Turbulence Simulation Model," American Helicopter Society 59th Annual Forum Proceedings, Phoenix, AZ., 6-8 May, 2003.

12. Sahasrabudhe, V. et al., "Simulation Investigation of a Comprehensive Collective-Axis Tactile Cueing System," American Helicopter Society 58th Annual Forum Proceedings, Montreal, Canada, 11-13 June, 2002.

13. Williams, J. N., Ham, J. A., and Tischler, M. B., "Flight Test Manual: Rotorcraft Frequency Domain Flight Testing," U.S. Army Aviation Technical Test Center, Airworthiness Qualification Test Directorate, AQTD Project No. 93-14, September 1995.

14. Howlett, J. J., "UH-60A Black Hawk Engineering Simulation Program: Volume I – Mathematical Model," NASA CR-166309, December 1981.

15. Tischler, M. B., Colbourne, J., Morel, M., Biezad, D., Cheung, K., Levine, W., and Moldoveanu, V., "A Multidisciplinary Flight Control Development Environment and Its Application to a Helicopter," IEEE Control Systems Magazine, Vol. 19, No. 4, August 1999, pp. 22-33.

16. Tischler, M. B., Fletcher, J. W., Morris, P. M., and Tucker, G. E., "Flying Quality Analysis and Flight Evaluation of a Highly Augmented Combat Rotorcraft," Journal of Guidance, Control, and Dynamics, Vol. 14, No 5, pp. 954-964, September-October 1991.

17. Crawford, C. C., "Potential for Enhancing the Rotorcraft Development/Qualification Process using System Identification," RTO SCI Symposium on System Identification for Integrated Aircraft Development and Flight Testing, Madrid, Spain, 5-7 May 1998.

18. Colbourne, J. D., Frost, C. R., Tischler, M. B., Cheung, K. K., Hiranaka, D. K., and Biezad, D. J., “Control Law Design and Optimization for Rotorcraft Handling Qualities Criteria Using CONDUIT,” American Helicopter Society 55th Annual Forum Proceedings, Montreal, Canada, 25-27 May, 1999.

19. Blanken, C. L., Cicolani, L., Sullivan, C. C., and Arterburn, D. R., “Evaluation of Aeronautical Design Standard – 33 Using a UH-60A Black Hawk,” American Helicopter Society 56th Annual Forum Proceedings, Virginia Beach, VA, 2-4 May 2000.

20. Cooper, G. E. and Harper, R. P., “The Use of Pilot Rating in the Evaluation of Aircraft Handling Qualities,” NASA TN D-5153, April 1969.

21. Sahasrabudhe, V. et al., “Modernized Control Laws: From Design to Flight Test,” AHS 4th Decennial Specialist's Conference on Aeromechanics, San Francisco, CA, 21-23 January 2004.